DETECTION OF EARTH SURFACE DISPLACEMENTS IN AREA OF INTENSIVE OIL PRODUCTION BY RADAR INTERFEROMETRY

405

Anton V. Filatov [1]

[1] Ugra Research Institute of Information Technologies, 151 Mira St.,
Khanty-Mansiysk, 628011, Russia, +73467359146, +73467359019, fav@uriit.ru

ABSTRACT

Given work describes features of interferometric processing of the radar data on territory of Western Siberia, and also application of obtained results for monitoring of displacements of a ground surface around the area of intensive oil and gas production. The scientific side of work consists in research, developing and realization of methods of processing of radar measurements in the conditions of high temporal decorrelation. The practical side is connected with monitoring of a surface of oil and gas deposits and detection of motions caused by hydrocarbons extraction. During research work ALOS\PALSAR data were used. As a result of InSAR processing maps of relative seasonal displacements on territory of Samotlor oilfields were constructed. The estimation of applicability of C-band and L-band radar data based on coherence distribution is made. On the basis of ALOS\PALSAR data maps of long-term displacements on territory of Samotlor oilfield and Gubkin gasfield are made. The results of InSAR processing are verified with the materials of ground leveling on geodynamic polygons.

1. INTRODUCTION

As a result of the spatial analysis of breakdown susceptibility of pipelines in connection with a site of local breaks it has been established, that a repeating breakdown susceptibility of oil pipelines is dated for these local breaks. From the point of view of physics and the geomechanics, studied structures prove as dynamically deformation processes, however without explosive infringements of thickness of breeds. Many researches show, that influence of local breaks of an earth crust on pipelines considerable, and can lead to destruction of pipelines. The importance of the given work is defined by necessity of decrease breakdown susceptibilities of oil and gas pipelines [1]. At the same time Earth surface displacements monitoring in oil and gas fields areas is regulated by "The Instruction on Surveying Operations. RD-07-603-03" by Gosgortechnadzor (Russian State Engineering Supervision Instance). This monitoring must include creation of the fixed reference points system both in limits of hydrocarbon field contour and outside of it (i.e. in the area of possible man-caused deformation and outside of this area). Traditional methods of regular measurements (mostly 2nd class leveling) should be applied on this system of points. Differential radar interferometry is an effective method for estimation of plane and vertical displacements in big areas caused by breakdown structure movements. High cloudiness and snow period duration caused by location of investigated territory in north latitudes make difficulties for monitoring of ground surface by optical remote sensing data. At the same time nature landscape features presented in that area place a certain limitation on interferometric processing and require more detailed data analysis. The main objective of the research work is construction of displacements maps of ground surface and detection of subsidences that have a negative impact on objects of oil and gas production. The complex of the researches spent using remote sensing data is addition to the land geological and geophysical works which are carried out by oil-extracting companies.

2. METHOD

Principles of interferometric processing.
The method satellite radar interferometry uses effect of an interference of electromagnetic waves and is based on mathematical processing of several coherent amplitude-phase measurements of the same site of ground surface with shift in space of the receiving antenna of radar. Two or more images received by the sensor at repeated flight of the space vehicle over the same territory are used for this purpose. As a result of manipulation with phase components of radio signals it is possible to obtain elevation of one resolution element relative to another from what further to construct digital elevation model with reference to reflective surface, and also to estimate the changes of the elevation which have happened in time between acquisitions.

The method of interferometric processing is a powerful tool which is well described in many books and papers [2-6]. The short description of principles of radar interferometry made on the basis of the used scientific literature is given below.

The interferogram is generated by multiplication of two radar images presented in complex values:

$$I = S_1 \cdot S_2^* = A_1 e^{j\phi_1} \cdot A_2 e^{-j\phi_2} = A_1 A_2 \cdot e^{j(\phi_1 - \phi_2)} = A_1 A_2 \cdot e^{j\Phi}$$

где I is the complex interferogram, S_1 is the radio signal in complex values received during first (master) acquisition, S_2^* is the complex-conjugate signal received during second (slave) acquisition, A_1, A_2 are amplitudes of the signals, ϕ_1, ϕ_2 are phase values of the signals, Φ is the resultant interferometric phase.

The interferogram phase consists of several components:

$$\Phi = \Phi_{topo} + \Phi_{def} + \Phi_{atm} + \Phi_n \qquad (1)$$

where Φ_{topo} is the phase contribution due to topography observation under two different angles, Φ_{def} is the phase contribution due to surface displacement in time between acquisitions, Φ_{atm} is the phase contribution due to difference of optical ways lengths because of refraction in the environment of signal propagation, Φ_n is phase variations as a result of the speckle-noise caused by incomplete compensation of a phase of multiple reflections due to reorientation of elementary objects and their movements inside of a resolution element.

The geometrical scheme of calculation of altitude of ground surface (H) and displacement (Δh) in time between acquisition is given in the Fig. 1. The used method of interferometric processing allows to determine the given values on the basis of known arguments: a satellite position during first acquisition (H_{sat}); a relative positioning of satellites at multitemporal acquisitions (length and attitude of a baseline B); a difference of distances from the antenna of a radar to a point on ground surface at repeated acquisitions ($R_1 - R_2$).
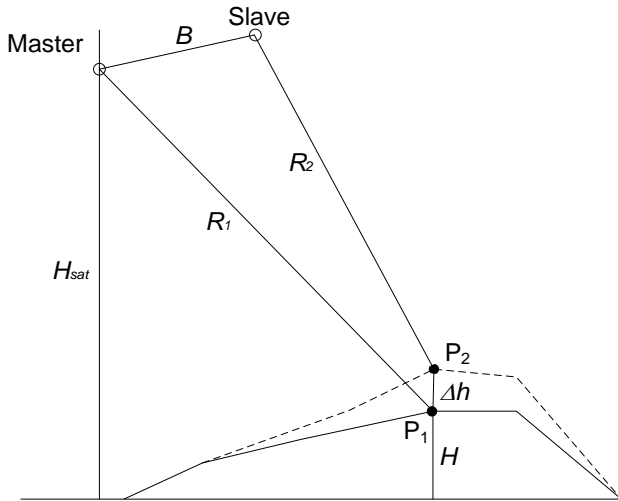
Fig. 1 Interferometric configuration of two-pass radar acquisition

The topographic component of an interferometric phase depends on the relative height of a site of ground surface:

$$\Phi_{topo} = -\frac{4\pi}{\lambda}\frac{B_\perp}{R\sin\theta}H + \Phi_{flat} \qquad (2)$$

where λ is the wavelength of the sensing signal (0.23m for used PALSAR data), $B_\perp$ is the perpendicular (normal) projection of the baseline, R is the distance between satellite position during first acquisition and point on ground surface, θ is the incidence angle, H is the height of a site of ground surface over a reference ellipsoid, Φ_{flat} is the predetermined phase calculated from model of a reference ellipsoid.

The phase component Φ_{def} is proportional to displacement Δh of a site of ground surface in time between acquisitions in a line-of-sight direction:

$$\Phi_{def} = \frac{4\pi}{\lambda}\Delta h \qquad (3)$$

Instruments, defining orbital arguments of satellite motion, allow to evaluate a position (H_{sat}) accurate within 1m [7].

The difference of distances from the antenna of a radar to a point on ground surface is determined as a phase difference of the radar signals received at repeated acquisitions. Sensor PALSAR allows to determine plane co-ordinates of a site of ground surface to within 9.7m [8]. To correlate the produced radar measurements with a site of ground surface which one in time between acquisitions in addition to all modified its position from P_1 on P_2, co-registration and resampling of radar data are carried out. With the help of subpixel co-registration accuracy of radar frames overlapping reaches $1/10^{th}$ of spatial resolution (~10m for PALSAR data).

The radar interferometry singularity consists in calculation of altitudes and displacements of sites of a surface relative to concerning adjacent, therefore computational values are a little subject to influencing of orbital errors. Only length and orientation of a baseline (B) exactly their variation along the satellite orbit can introduce a notable error to the end results. Using additional ground terrestrial reference points for baseline refinement, it is possible to make bring accuracy of its determination to 1mm.

Standard chain of the stages executed during interferometric processing:
- source images co-registration;
- interferogram generation;
- interferogram flattening;
- interferogram filtering;
- coherence map generation;
- interferometric phase unwrapping;
- unwrapped phase editing;
- baseline refinement;
- relative heights computation;
- relative displacements computation.

For elimination of a topographic component in the process of differential interferometry as reference digital elevation models accessible data GTOPO 30, ASTER GDEM, the digitized topographic maps of scale 1:50000 were used. SRTM (Shuttle Radar Topography Mission) don't exist for this territory.

Also the configuration of radar frames during 4-pass acquisition was used:

$$\Phi_1 = H*K_1 + V*T_1*\frac{4\pi}{\lambda}$$
$$\Phi_2 = H*K_2 + V*T_2*\frac{4\pi}{\lambda} \tag{4}$$

where Φ_1, Φ_2 are interferometric phases for first and second pairs respectively, K_1, K_2 are height to phase conversion factors, T_1, T_2 temporal baselines of first and second pairs respectively [9].

Selection of source data for interferometric processing.
In the research work PALSAR data of two observations modes were used:
- Fine Beam Single (FBS): spatial resolution ~5m range, 4.5m azimuth, acquisition during snow season;
- Fine Beam Dual (FBD): spatial resolution ~10m range, 4.5m azimuth, acquisitions during snowless season [7].

Only HH (radiating and receiving and horizontally polarized signal) polarization mode were used.

For construction of digital elevation models and calculation of displacements it is necessary to select and order pairs of radar frames with certain arguments of sensing. Critical values in this case are temporal and spatial baselines. Increasing of the first parameter leads to lowering of coherence of radar measurements occurring at different times owing to variations of a vegetative cover and the dielectric properties of reflective surface. Increasing of the second parameter leads to increasing of part of topographic contribution of interferometric phase proportional to reflective surface altitudes.

Radar interferometry method is based on processing of coherent signals reflected from ground surface at various times. The coherence value (from 0 to 1) mirrors the level of corrupting of the interferogram, is calculated as correlation of two signals in complex values and is a standard of operability of pair of frames for the further processing.

$$\gamma = \frac{S_1 S_2^*}{\sqrt{S_1 S_1^* \cdot S_2 S_2^*}} \tag{5}$$

where S_1, S_2 are the complex values of reflected signals for master and slave frames.

Decrease of signals coherence is promoted by some factor (sources of decorrelation):

$$\gamma = \gamma_{geom} \times \gamma_{vol} \times \gamma_{temporal} \tag{6}$$

where γ_{geom} is the spatial (geometrical) decorrelation as a result of difference of ground observation angles during the repeat passes sensing, γ_{vol} is the volume decorrelation caused by propagation of radar signals through growth, $\gamma_{temporal}$ is the temporal decorrelation due to changes of reflective properties of objects and their reorientation inside the resolution element.

For C-band synthetic aperture radars observation carried out during late spring, summer and early autumn seasons is acceptable for interferometric processing [10]. The maximum temporal baseline value at which one there is no interferogram decorrelation amounts 70 days. The distance between a radar antenna at repeated orbits should not exceed 600m, otherwise it leads to corrupting of an interferometric phase caused by spatial decorrelation. It is necessary to note that critical value of normal baseline length for ENVISAT\ASAR (with incidence angle 23° and spatial resolution 30м) amounts 1.1km.

Coherence comparing between pairs of frames received by ENVISAT\ASAR and ALOS\PALSAR and also between ALOS\PALSAR pairs is carried out under various conditions of observation. Co-registration of different coherence maps was based on geocoding using orbital data and observation parameters. Comparing showed that owing to longer wavelength (0.23m) and as consequence higher penetrating effect correlation of ALOS\PALSAR interferometric pairs is considerably higher. This conclusion is confirmed by comparing of coherence maps based on interferometric pairs of frames on territory of the Fedorov oilfield given in Tab. 1. Mean value of coherence of ALOS\PALSAR pair is higher despite spatial decorrelation as a result of significant length of the normal baseline value.

Table 1 Comparing of mean coherence of ENVISAT\ASAR and ALOS\PALSAR interferometric pairs acquired in summer seasons with minimal temporal baseline

Sensor	Master	Slave	$B_\perp$,m	γ
ASAR	10.07.2004	14.08.2004	60	0.319
PALSAR	12.06.2008	28.07.2008	2323	0.451

Comparing of coherence maps (Tab. 2) of ALOS\PALSAR pairs on territory of the Samotlor oilfield with different spatial baselines, showed the high corrupting of phase of the interferogram owing to spatial decorrelation. In this connection it is not possible to construct digital elevation model of wood territory for which one pairs with a baseline more than 3000m are used [11].

Table 2 Comparing of mean coherence of ALOS\PALSAR interferometric pairs with long and short normal baseline

Sensor	Master	Slave	$B_\perp$,m	γ
PALSAR	19.08.2007	04.10.2007	419	0.584
PALSAR	06.07.2008	21.08.2008	3465	0.251

Moreover coherence of an interferometric pair with length normal baseline more than 3000m decreasing with increasing of incidence angle. Mean value of coherence at

far-range observation area is less by 0.134 than at near-range zone therefore accuracy of height reconstruction reduces with moving away from sensor antenna..

Unlike ENVISAT\ASAR data for ALOS\PALSAR interferometric pairs (Tab. 3) during observation of snow surface it is possible to generate stable (informative) interferogram even with temporal baseline more than 1 year. Values of deformations obtained as a result of interferometric processing of winter season acquisitions reflect movements of earth crust block more accurately due to small influence of seasonal changes of peat bogs surface level.

Table 3 Comparing of mean coherence of ALOS\PALSAR interferometric pairs acquired at snow and snowless seasons.

Sensor	Master	Slave	$B_\perp$,m	γ
PALSAR	19.08.2007	04.10.2007	419	0.533
PALSAR	18.12.2007	02.02.2008	789	0.471
PALSAR	04.10.2007	06.07.2008	1954	0.156
PALSAR	30.01.2007	18.12.2007	2731	0.266

Thus, application of data acquired with synthetic aperture radar with high wavelength (ALOS\PALSAR, 0.23m) eliminates small vegetative covers masking influence and allow generating interferogram more inconvertible against temporal decorrelation. High accuracy of digital elevation models is reached because of usage of interferometric pairs of snowless surface with incidence angle from 36.6° to 38.7° (near-range). To estimate long-term ground surface displacements PALSAR data acquired at any season can be used. But the temporal baseline can't exceed 4 years.

Application of corner reflectors and anthropogenous objects for geocoding.

Ground reference points setting conformity between a pixel on radar image in azimuth and slant range coordinates and a reflective object on ground surface in geographic projection coordinates are applied to increase accuracy of geocoding. For territory of the city of Khanty-Mansiysk which one was the test site during research work checkout of capability of detection of the trihedral corner reflector with edge length 1.25m on PALSAR imagery (Fig. 2). Under condition of a minimal backscattering from background surface such corner reflector is probably to detect on a PALSAR frame.

Placing of enough of corner reflectors with edge length enough for detection on the radar image on the long-lived period in the conditions of an inaccessible terrain is labour-intensive and cost intensive process. The basic problem consists in delivery and installation of corner reflectors to an oilfield. Analysis of the amplitude component of radar images received from satellites ERS-2, ENVISAT, ALOS, TerraSAR-X, revealed high backscattering from oil production objects. For oil

extraction on territory of license districts the large quantity of multiple-well platforms is disposed.

Fig. 2 Trihedral corner reflector (1.25m) installed on the test site of the city of Khanty-Mansiysk and aimed on ALOS\PALSAR ascending acquisitions

Fig. 3 Objects of typical multiple-well platform

On each multiple-well platform which one is presented in the Fig. 3 mining rotary balanced jacks and other concomitant objects are disposed. Each metal object which is located on territory of a multiple-well platform represents the technogenic corner reflector and is dedicated with a bright point on a radar image. Standard electric control unit of rectangular form has backscattering level 12 times higher then background.

During subsatellite measurements in terrain of oil and gas fields of Khanty-Mansiysk autonomous okrug using GPS receiver coordinates of ground control points were determined. These coordinates are used to improve geocoding of PALSAR radar images.

Method of interferogram processing in case of high temporal decorrelation.

After interferogram filtering stage phase unwrapping (addition of $2\pi k$ value where k is an positive or negative integer number) is carried out. However significant noise level due to high temporal decorrelation leads to incorrect algorithm functioning and so unwrapped interferogram contains phase discontinuities. In the presented research work to reconstruct absolute phase 3 interferograms generated with consistent multilook window size were used. Unwrapped interferograms is corrected under formula presented below.

$$\Phi_{11,c}(i,j) = \Phi_{11,abs}(i,j) \bmod 2\pi + 2\pi \left[\Phi_{33,abs}(i,j)/2\pi\right]$$
$$\Phi_{22,c}(i,j) = \Phi_{22,abs}(i,j) \bmod 2\pi + 2\pi \left[\Phi_{33,abs}(i,j)/2\pi\right] \quad (7)$$

where $\Phi_{11,c}$ and $\Phi_{22,c}$ are adjusted phase values; mod denotes means residue of division; [ ] denotes the integer part; $\Phi_{11,abs}, \Phi_{22,abs}, \Phi_{33,abs}$ are unwrapped phase values obtained from interferograms generated with 1x1, 2x2 and 3x3 multilooking respectively; i is the azimuth pixel index; j is the slant range pixel index. The given formula has correct result provided that during multilooking fringe integrity has not been upset.

The final phase value $\Phi_{fin}(i,j)$ at each pixel is selected on the basis of coherence map.

$$\Phi_{fin}(i,j) = \begin{cases} \Phi_{33,abs}(i,j), & \gamma_1 > \gamma(i,j) \ge \gamma_{cr} \\ \Phi_{22,c}(i,j), & \gamma_2 > \gamma(i,j) \ge \gamma_1 \\ \Phi_{11,c}(i,j), & \gamma(i,j) \ge \gamma_2 \end{cases} \quad (8)$$

wheres $\gamma(i,j)$ is the coherence value at the point with i and j coordinates; $\gamma_{cr}, \gamma_1, \gamma_2$ are thresholds coherence values ($0 < \gamma_{cr} < \gamma_1 < \gamma_2 < 1$).

The threshold values are based on analysis of the coherence distribution over the scene area. As a result the final interferogram contains areas with different spatial resolution and height accuracy. During PALSAR data processing next defaults threshold coherence values are set $\gamma_2 = 0.25, \gamma_1 = 0.15, \gamma_{cr} = 0.1$ which can be changed depending on decorrelation influence.

Persistent scatterer interferometric processing.

Temporal and baseline decorrelation factors and atmospheric inhomogeneities does not allow classic radar interferometry approach to became an effective mathematic instrument for monitoring of ground surface deformations occurred during long-lived period (more than 3 years).

Due to temporal decorrelation interferometric measurements for areas with dense vegetation and for sites where electromagnetic properties and-or positions of elementary reflectors inside the resolution cell are changed in time become impossible.

Geometric decorrelation limits quantity of interferometric pairs which can be used in processing. Atmospheric inhomogeneities create a phase shift which one is superposed with each radar image and reduces accuracy of displacement estimation. Besides atmospheric phase shift generates slow phase change within a radar scene depending on water vapour distribution and cannot be valued and eliminated on the basis of the coherence map.

Persistent Scatterer Interferometry (PSI) approach was developed at Politecnico di Milano in 1999 and is well described in science literature. Advantages of this approach are based on specific properties of point objects that keep high level of the radar signal backscattering during many repeated multitemporal acquisition [12 - 14]. Often size of such point reflective object is less than resolution cell therefore coherence is high enough (γ >0.5) even for pairs of frames with spatial baseline more then the critical value. In the condition that atmospheric phase shift was estimated and eliminated heights of persistent scatterers above the reference surface can be reconstructed with accuracy better than 1m and displacements precision is better than 1cm.

For monitoring of petroleum objects located on territory of oilfields of Khanty-Mansiysk autonomous okrug method of persistent scatterers interferometric processing described at the paper [12] was realized. This approach contains algorithms of master and slaves scenes selection, persistent scatterers detection and calculation of atmospheric phase shift, heights and displacement velocities.

Three main moments that were used in this research work are presented below.

PSI approach used $K+1$ multitemporal radar images of the observable site of ground surface. One of them is selected as a master and others K are referenced as slaves and K interferograms are generated. Selection of master scene is based on minimization of influence of factors that reduce interferometric coherence.

$$\gamma_m = \frac{1}{K}\sum_{k=0}^{K} g(B_{k,m}, B_{cr}) \times g(T_{k,m}, T_{cr}) \times g(fdc_{k,m}, fdc_{cr}) \quad (9)$$

where

$$g(x,c) = \begin{cases} 1 - |x|/c & \text{при } |x| < c \\ 0 & \text{при } |x| \ge c \end{cases}$$

where $B_{k,m}$, $T_{k,m}$ and $fdc_{k,m}$ are the values of the normal baseline, the temporal baseline and the mean Doppler centroid frequency difference of each pair of frames; B_{cr}, T_{cr}, fdc_{cr} are the critical values of given parameters.

Initial scene m with maximum value of γ_m is selected as a master [14].

The next stage is selection of points which can be persistent scatterers.

An object can be a candidate of persistent scatterer if it has high and stable backscattering level (pixel amplitude), than phase of the radar signal received from such object has low dispersion. Standard approach based on coherence map is useless due to:

- compex interferometric coherence is subjected to influence of spatial baseline variations and reference elevation model errors;

- during coherence map generation averaging of values within moving running window is carried out and so individual points can be lost.

Another approach consists in using the condition of pixel amplitude stability.

$$\sigma_v \boxempty \frac{\sigma_A}{m_A} \boxempty D_A \qquad (10)$$

where σ_v is the phase dispersion value; σ_A is the amplitude dispersion value; D_A is the dispersion index.

For persistent scatterers candidates selection the threshold value is set to $D_A < 0.25$. The main condition is that amplitude images should be radiometricaly corrected and normalized.

Further processing is carried out for K interferometric pairs and for H individual pixels represented as persistent scatterers. Estimation of atmospheric phase shift, heights and displacement velocities is carried out in accordance with next system of equations.

$$\Delta\vec{\Phi} = \vec{a}1^T + \vec{p}_\xi \vec{\xi}^T + \vec{p}_\eta \vec{\eta}^T + \vec{B}\Delta\vec{q}^T + \vec{T}\vec{v}^T + \vec{E} \qquad (11)$$

where

- $\Delta\vec{\Phi}[K \times H]$ are differential interferometric phase values;

- $\vec{a}[K \times 1]$ are constant phase values;

- $\vec{p}_\xi[K \times 1]$ and $\vec{p}_\eta[K \times 1]$ contain the slope values of the linear phase components, along the azimuth $\vec{\xi}[H \times 1]$ and slant range $\vec{\eta}[H \times 1]$ direction due to atmospheric phase contributions and orbital fringes;

- $\vec{B}[K \times 1]$ contains the normal baseline values (referred to the master image). For large areas, $\vec{B}$ cannot be considered constant, and the array $\vec{B}[K \times 1]$ may become a matrix $\vec{B}[K \times H]$;

- $\Delta\vec{q}[H \times 1]$ contains phase vales proportional to the elevation of each persistent scatterer;

- $\vec{T}[K \times 1]$ contains the time interval between K slave images and the master one;

- $\vec{v}[H \times 1]$ contains slant range velocities of the persistent scatterers;

- $\vec{E}[K \times H]$ contains residues that include atmospheric effects different from constant and linear components in azimuth and slant range direction, phase noise due to temporal and spatial decorrelation, and the effects of possible random pixel motion.

As formulated in (11), the problem would be linear if the unwrapped values of matrix phase $\Delta\vec{\Phi}$ were available. We have $H \cdot K$ equations and $3K + 2H$ unknowns: $\vec{a}$, $\vec{p}_\xi$, $\vec{p}_\eta$, $\Delta\vec{q}$, $\vec{v}$. Data are $\Delta\vec{\Phi}$, $\vec{\xi}$, $\vec{\eta}$, $\vec{B}$, $\vec{T}$. Thus, in principle, (11) could be inverted to get the local topography, the velocity field, and constant and linear phase contributions. In practice, however, we face a nonlinear system of equations (phase values are wrapped modulo 2π) to be solved by means of an iterative algorithm, and an available digital elevation model should be exploited to initialize the iterations. Reference digital elevation model is used for interferogram flattening and reducing known topography.

The nonlinear system of equations (11) can be solved provided that:

1) the signal to noise ratio is high enough (i.e., the H selected pixels are only slightly affected by decorrelation noise);

2) the constant velocity model for target motion is valid;

3) the atmospheric phase shift distribution over the research area can be approximated as a phase ramp.

The convergence depends on the following factors:

1) space-time distribution of the acquisitions (which should be as uniform as possible: spatial and/or temporal "holes" in the data set should be avoided);

2) reference digital elevation model accuracy ($\Delta\vec{q}$ should generate small phase contributions for low $\vec{B}$);

3) dimensions of the area of interest (atmospheric phase shift distribution and orbital fringes should be well approximated by linear phase components);

4) target motion should be slow enough to avoid aliasing and be well approximated by the constant velocity model. For convergence, $\vec{v}$ should generate small phase contributions for low $\vec{T}$.

Used software.

In the course of research work as a main interferometric processor software module SARscape developed by SARMAP company and geoinformation system ENVI developed by ITT VIS company were used. Additional processing was realized using mathematical programming environment MATLAB developed by MathWorks company. Following MATLAB scripts were developed:

- the program for eliminating small (less than 100 pixels) coherent sites of a filtered interferogram based on coherence map analysis;

- the program for height calculation for areas of digital elevation model with low coherence based using interpolation based on boundary values;

- the program for solving system (11) and estimating of displacement velocities of persistent scatterers.

3. RESULTS

Areas of interest

Regions selected for research are either great oil and gas fields or important oil and gas production objects (Fig. 4). Also significant argument was availability of additional data and earlier made investigations.
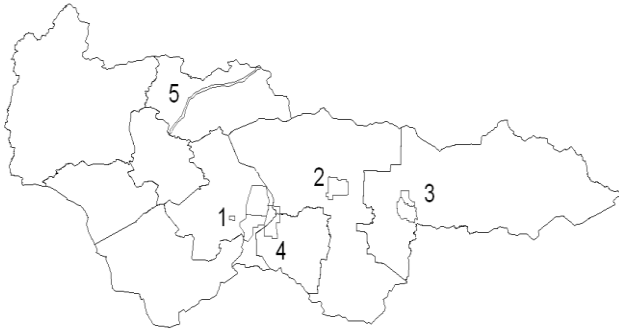
Figure 4. Research regions

Areas in the Fig. 4 are marked by numbers:
1) The city of Khanty-Mansiysk;
2) Fedorov oilfield;
3) Samotlors oilfield;
4) Priobskiy and Prirazlomniy oilfields;
5) Beloyarskiy pipeline.
First area were used as a test polygon for different methods and ideas checking.

More detail processing was carried out for Samotlor oilfield and additional Gubkin gasfield located in Yamalo-Nenetskiy autonomous okrug. On territory of this deposits geodynamic polygons were developed and much volume of additional ground measurements data is available.

Digital elevation models on the territory of major oil and gas fields of West Siberia region

Using PALSAR data acquired during 2007-2010 digital elevation models of all research regions were constructed one of them is presented in Fig. 5.

During interferometric processing and digital elevation model generating correction using ground reference control points was carried out. Triangulation points and height marks presented on topographic maps of scale 1:50000 were used as ground reference points. Digital elevation model of ground surface generated using this approach reflects height of relief taking into account envelope of vegetation covers predominant on this territory.

All digital elevation models were converted from radar azimuth slant range coordinates to Universal Transverse Mercator projection with proper zone. Heights accuracy is 10m. Pixel spacing is 20m.
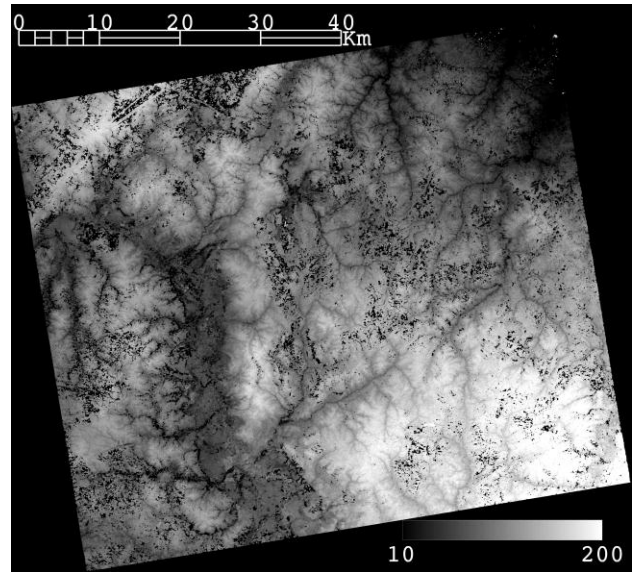
Fig. 5 Digital elevation model of territory of Beloyarskiy trunk pipeline

Mapping of seasonal ground surface displacements on territory of exploited oil fields

In spring, summer and autumn season level of peat bogs presented on territory of West Siberia region is changed, as a consequence displacement of reflective surface is happened. In case of long-term deformations monitoring such seasonal movements have masking effect and does not allow to detect small vertical shifts caused by oil extraction [15].

Interferometric pairs ENVISAT\ASAR and ALOS\PALSAR on territory of Fedorov and Samotlor oilfields with minimum temporal baseline (46 days) and short normal baseline (about 300m) were processed. 3-pass differential interferometry approach was used and reference digital elevation model is based on PALSAR data.

As a result of differential interferometric processing of PALSAR data mapping of seasonal displacements on surface of peat bogs was done. Positive and negative shifts up to 4cm for 46 days were fixed. It is established that negative displacements are connected with discharge of bog in a river network and positive displacements are connected with raising of level of subsoil water in peat bogs in the field of internal drain and anthropogenic sites.

Combined analysis of PALSAR and LANDSAT-7/ETM optical images was carried out. An abundance of water observed on optical image indicates drainless areas on peat bogs. Displacements on peat bogs caused by water level interseasonal fluctuations were confirmed during the ground investigations in October, 2007. It is well appreciable in photos of oil spills appeared after pipeline damage.

Such short-period displacements make negative impact on oil and gas pipelines and raise their breakdown susceptibility. Comparison of calculated displacements

with the scheme of dynamically stress zones constructed by science center "Geoecology" (Surgut) on a basis of lineament analysis using optical satellite images is carried out. The raised breakdown susceptibility of oilfield pipelines in places of crossing with dynamically stress zones can be connected with the seasonal displacements of ground surface which have been detected by the radar interferometric method.

Monitoring of long-term displacements on territory of Samotlor geodynamic polygon
According to the ecological program "Complex system of geodynamic safety in the license area of Samotlor oilfield" closed company scientific production association "Center of applied geodynamics" the Samotlor geodynamic polygon has been being developed during 2001-2002 years.
Since 2002 yearly in summer season on the geodynamic polygon leveling, GPS-measurements and gravitational survey is carried out. West Siberian Branch of Institute of Petroleum Geology and Geophysics of the Siberian Branch of Russian Academy of Science carries out mining and ecological monitoring of claim of Samotlor oilfield [16].
In spite of great amount of deep reference markers (104 monuments) installed on the geodynamic polygon point ground measurements allow to do plane estimation only using additional interpolation. Therefore during 2008-2011 interferometric processing of PALSAR data was carried out in order to construct displacement map of Samotlor oilfield.
In table 4 processed interferometric pairs are presented, 3-pass approach were used.

Table 4 PALSAR interferometric pairs on territory of the Samotlor oilfield during 2007-2009 years

Master scene ID	Slave scene ID	$B_\perp$,m
Reference digital elevation model (T = 46 days)		
ALPSRP130501220	ALPSRP137211220	3427
Displacements maps (T = 1 year)		
ALPSRP076821220	ALPSRP130501220	1362
ALPSRP130501220	ALPSRP184181220	466

Results of differential interferometric processing of radar scenes from Table 4 are presented in Fig. 6, 7, 8 in the form of spatial profiles which one demonstrate displacements on the Samotlor oilfield over the subsidence mould. Combination of spatial profiles based on results of processing of radar frames for 2007-2008 and 2008-2009 allows to trace deformation dynamics during 2 years.
Radar interferometry method is based on processing of coherent multitemporal signals reflected from ground surface. Therefore sites of interferogram with low coherence contains significant noise volume. Moreover due to specificity of natural landscapes of West Siberia

region radar signal reflects not from mineral ground but from peat bogs surface. At the same time vegetation cover change reduces coherence of multitemporal radar signal [17]. Due to noise effect calculated displacements (solid line) along spatial profiles contain random component (Fig. 6, 7). Interpolation of deformation values with 6th degree polynom allow to mark smooth curve (dash line on Fig. 6, 7).
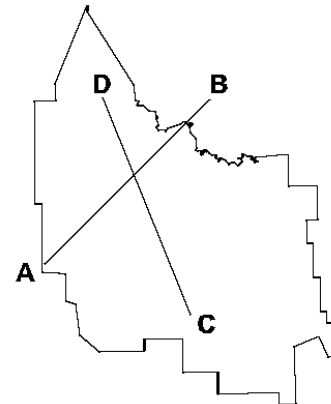
Fig. 6 Position and direction of spatial profiles over subsidence mould on the Samotlor oilfield
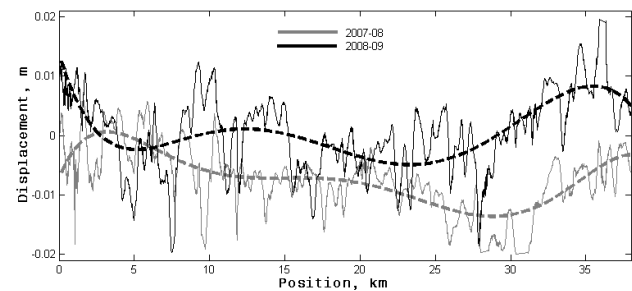
Fig. 7 Spatial profile AB
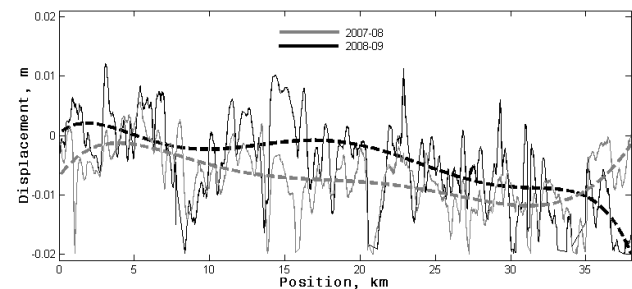
Fig. 8 Spatial profile CD

To construct smooth displacements map results of 2-dimension interpolation of individual values with coherence >0.75 can be used. Results of interferometric processing of scenes from table 4 presented in such form are shown in Fig. 9 and 10. White color contour marks zero isohyps of subsidence mould. Materials of high-accuracy geodetic surveying are presented as values in points and so maps based on them are constructed by

interpolation. In this connection form presented in Fig. 9 and 10 is the best way for analysis of such heterogeneous data.
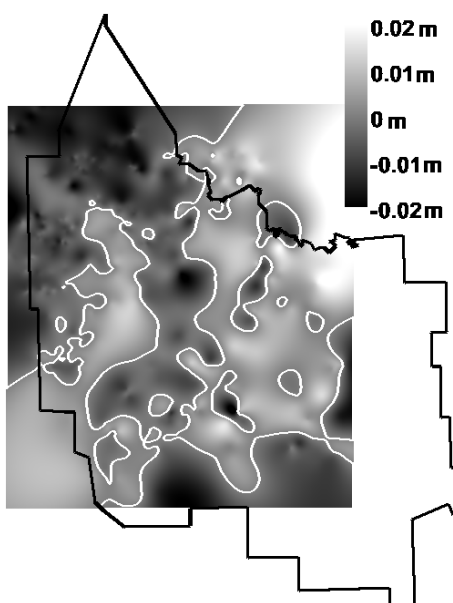
Fig. 9 Ground surface displacements map of the Samotlor oilfield during 2007-2008 (white line is the zero isohyps of subsidence mould)
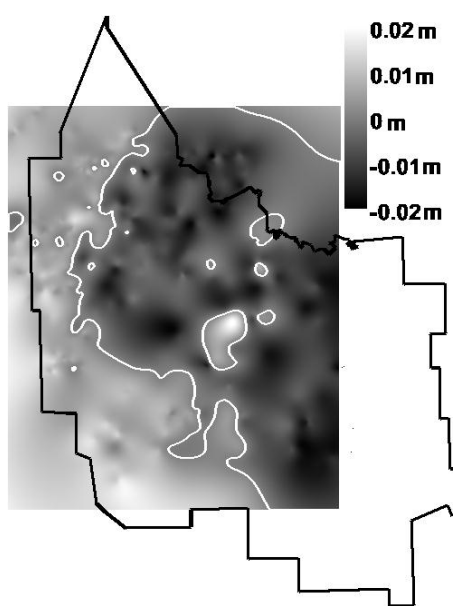
Fig. 10 Ground surface displacements map of the Samotlor oilfield during 2008-2009(white line is the zero isohyps of subsidence mould)

In 2009 and 2010 the problem of construction of displacements map of Samotlor oilfield and adjoining territory is set to estimate influence of adjacent oilfields on formation of subsidence mould. Additional task is improvement of vertical component accuracy. In summer seasons of 2009 and 2010 next 7th and 8th cycles of

geodetic operations on the Samotlor geodynamic polygon points including 2nd grade of accuracy leveling and gravimetric and GPS measurements was carried out. Additionally differential interferometric processing of radar data was made. As materials for interferometric processing 59 scenes of ALOS\PALSAR data covered Samotlor oilfield and adjacent territory were used. As a result of differential interferometric processing 6 displacements maps covering research area were constructed. To obtain absolute values of ground surface displacements height changes fixed on the Samotlor geodynamic polygon points from 2008 till 2009 were used. For territory without geodetic measurements ground control points with zero displacement were used [18].

In the Table 5 interferometric pairs used during construction of final digital elevation models and displacements maps are presented. In the Fig. 11 reference points used during digital elevation models and displacements maps construction. Symbols (*) indicates points which values were obtained during high accurate ground measurement on Samotlor geodynamic polygon. Symbols (+) indicates points obtained from topographic maps. Displacements of the (+) points have zero value.

Table 5 PALSAR interferometric pairs on territory of the Samotlor oilfield during 2007-2010 years

Master scene ID	Slave scene ID	$B_\perp$,m
Reference digital elevation model (T = 46 days)		
ALPSRP130501210	ALPSRP137211210	3457
ALPSRP130501220	ALPSRP137211220	3468
ALPSRP130501230	ALPSRP137211230	3478
ALPSRP132251210	ALPSRP138961210	3233
ALPSRP132251220	ALPSRP138961220	3245
ALPSRP132251230	ALPSRP138961230	3258
Displacements maps (T = 3 year)		
ALPSRP090241210	ALPSRP237861210	829
ALPSRP090241220	ALPSRP237861220	832
ALPSRP090241220	ALPSRP237861230	836
ALPSRP091991210	ALPSRP232901210	480
ALPSRP091991220	ALPSRP232901220	488
ALPSRP091991230	ALPSRP232901230	492
Displacements velocities of persistent scatterers, radar frames are acquired during 2007-2010		
ALPSRP208541220	ALPSRP054211220	1405
ALPSRP208541220	ALPSRP101181220	1328
ALPSRP208541220	ALPSRP107891220	2115
ALPSRP208541220	ALPSRP154861220	3297
ALPSRP208541220	ALPSRP161571220	2550
ALPSRP208541220	ALPSRP215251220	696
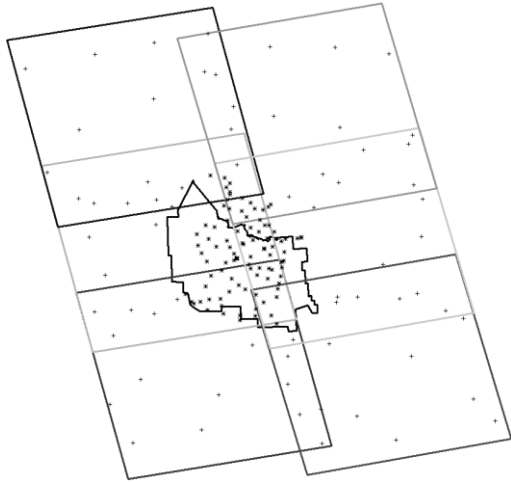
Fig. 11 Borders of displacements maps and ground control points distribution

In the Fig. 12 reference digital elevation model of research territory is presented. In the Fig. 13 and 14 displacement maps of research area is presented. Negative displacements inside the borders of the Samotlor license site form the subsidence mould and are connected with intensive oil extraction.
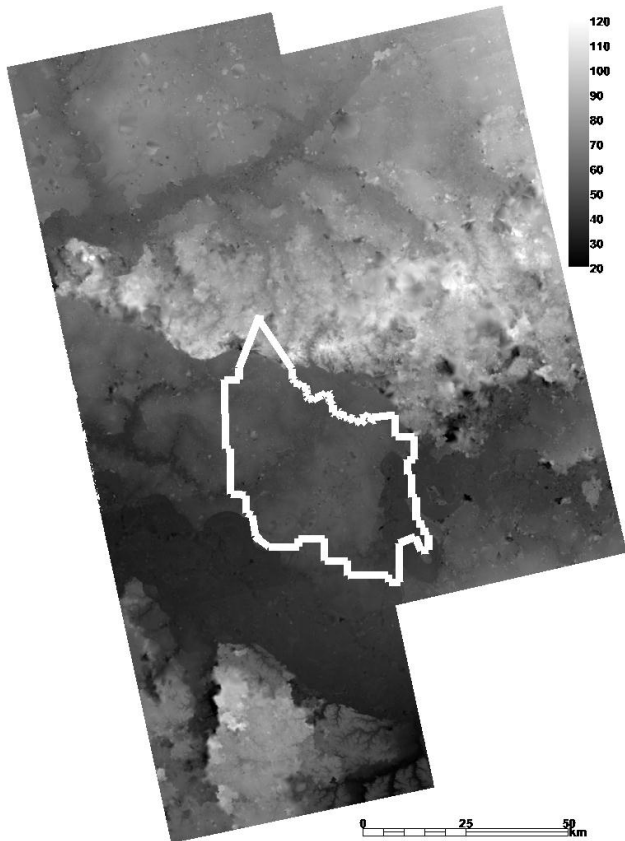
Fig. 12 Reference digital elevation model of the Samotlor oilfield and adjacent territories. Pixel spacing is 20m. Height accuracy is 10m. UTM projection, zone 43. Heights ramp is in meters.
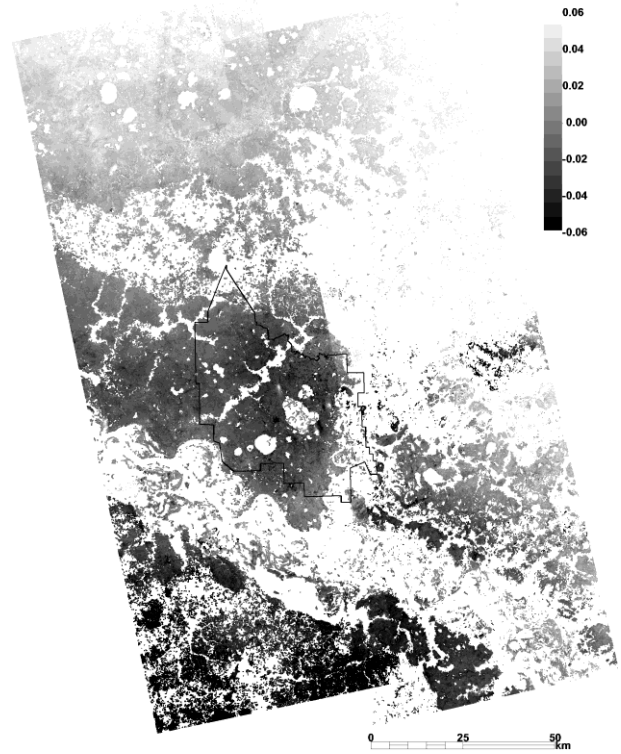
Fig. 13 Final displacements map of the Samotlor oilfield and adjacent territories for 2007-2010. Pixel spacing is 20m. Height accuracy is 0.02m. UTM projection, zone 43. Heights ramp is in meters.
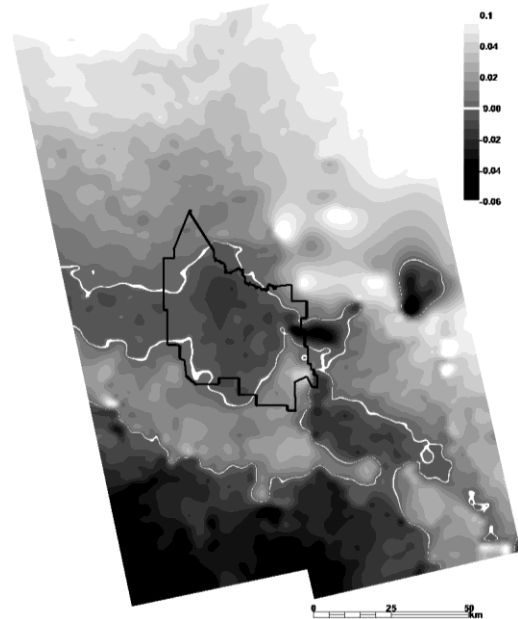
Fig. 14 Final displacements map of the Samotlor oilfield and adjacent territories for 2007-2010 obtained as a result of interpolation of individual high coherent values. Pixel spacing is 40m. Height accuracy is 0.02m. UTM projection, zone 43. Heights ramp is in meters. White line indicates zero isohyps of subsidence mould.

For checking of persistent scatterer interferometry approach described in previous section 7 PALSAR scenes acquired during 2007-2010 years (Table 5) were processed. Scene ALPSRP208541220 was selected as master and 6 differential interferogram were generated using SARscape software. ASTER GlobalDEM data were used as a reference digital elevation model. Height accuracy of these materials is 14m. As regions of interest territory of Izluchinsk GRES (thermal power station) and area of Izluchinsk settlement were selected that are located inside of the claim of the Samotlor oilfield. Size of the region of interest is 8x8km. 3365 points (persistent scatterers) were selected. After 118 steps of calculation heights, displacement velocities and atmospheric phase shift were obtained. Because of few used radar images areal estimation of displacement velocities has not been done. Obtained values can only indicate objects shift directions. Negative displacements of objects of Izluchinsk GRES and buildings located at Izluchinsk settlement were fixed [19].

Thus 3 cycles of interferometric processing of radar data on territory of the Samotlor oilfield were carried out. Mean error of displacement values is 2cm.

Zero values of isohyps of the subsidence mould based on materials of geodetic monitoring using shifts of reference points of Samotlor geodynamic polygon fixed during 2007-2010 are well correlated with results of differential interferometry. Conjectural zero isohyps of the subsidence mould in area without enough installed ground markers was corrected on the basis of results of PALSAR data processing. Central the most down part of the subsidence mould with displacement values from -10mm to -14mm are well correlated with interferometric measurements. Radar data also allow to make zero isohyps more accurate. As a result of combination displacements maps and materials of ground measurements interpretation 4 epicentres of negative deformations were detected. Such combination adds assurance in conclusions that subsidence zones are corresponded to anomalous areas of Earth masses concentration.

Using results of PALSAR data processing acquired in 2007-2010 displacements maps of territory of Gubkin gasfield were constructed. Ground measurements on the Gubkin geodynamic polygon were carried out only in 2000 and 2006 there is no additional information for processing. Deformations detected on Gubkin gasfield are from -3cm to +4cm during 2007-2008 and from -5cm to +7cm during 2007-2009. Tendency of positive and negative displacements of ground surface remain keeps during 3 consecutive cycles of measurements and so validity of deformation detection is confirmed.

Areas of subsidences and raisings are well correlated with areas of maximum hydrocarbon extraction volumes on Samotlor and Gubkin deposits.

4. DISCUSSION

Results of the given research work were discussed at three scientific technical meetings at TNK-BP SamotlorNefteGaz and also at scientific conferences in Russia and Europe.

Since results of differential interferometric processing has enough correlation with materials of interpretation of high accurate ground measurements displacements maps can be additional information during mining and ecological monitoring. Deformations based on radar data processing allow to reduce labour-intensive and expensive ground measurements. Frequency of accurate 2nd class leveling can be reduced to 1 in 5 years. Only GPS measurements should be carried out every half a year. Results of radar data processing by persistent scatterer interferometry approach with 5mm accuracy are a key and perspective of geodynamic monitoring of regions of intensive oil and gas extraction.

5. CONCLUSION

1) Optimum conditions of selection of radar data for generation of interferograms with low noise contribution were developed.
2) PALSAR L-band data has irrefutable advantage for research of specific landscapes of West Siberia.
3) Developed method of interferograms processing using different multilook window sizes allows to calculate height values in areas with high temporal decorrelation.
4) Metal objects located on territory of oil and gas fields can be used as technogenic corner reflectors for geocoding and to form net of persistent scatterers.
5) Digital elevation models on areas of intensive oil and gas extraction of West Siberia region were constructed.
6) Seasonal short-term peat bogs surface displacements were estimated.
7) Long-term deformations on territory of Samotlor and Gubkin deposits caused by earth crust block movements as a result of oil and gas extraction were estimated.
8) Developed methods and results of this research work were used as additional information during ecological monitoring.
9) 157 PALSAR scenes were used during research.

6. ACKNOWLEDGEMENT

6. REFERENCES

[1] A.O. Genush, "System analysis of oil field pipelines reliability in areas of influence of active tectonic structures at West Siberian oilfields", Ph.D. dissertation, Surgut State University, Surgut, Russia, pp. 1-20, 2005.

[2] H.A. Zebker, R.M. Goldstein, "Topographic Mapping Derived from Synthetic Aperture Radar Measurements", *Journal of Geophysical Research*, Vol. 91, pp. 4993-5002, 1986.

[3] A.K. Gabriel, R.M. Goldstein, and H.A. Zebker, "Mapping small elevation changes over large areas: Differential radar interferometry", *Journal of Geophysical Research*, Vol. 94, pp. 9183-9191, 1989.

[4] A. Ferretti, A. Monti-Guarnieri, and C. Prati, "InSAR Principles: Guidelines for SAR Interferometry Processing and Interpretation", ESA Publications, Noordwijk, 234 p., 2007.

[5] R. Bamler and P. Hartl "Synthetic aperture radar interferometry", *Inverse Problems*, Vol. 14, 54 p., 1998.

[6] R.F. Hanssen, "Radar Interferometry – Data Interpretation and Error Analysis", Kluwer Academic Publishers, Dordrecht, 308 p., 2001.

[7] "Information on ALOS PALSAR products for ADEN users", Technical Note ALOS-GSEG-EOPG-TN-07-0001, European Space Agency, 15 p., 2007.

[8] M. Shimada, O. Isoguchi, T. Tadono, and K. Isono, "PALSAR Radiometric and Geometric Calibration," *IEEE Trans. Geoscience and Remote Sensing*, Vol. 47, No. 12, pp.3915-3932, Dec. 2009.

[9] SARscape User Guide.

[10] A.V. Filatov and A.V. Yevtyushkin, "Monitoring of seasonal deformations of Earth surface by radar interferometry using ENVISAT\ASAR and ALOS\PALSAR data", *Proceedings of IV Scientific and practical conference "Inverse problems and informational technologies of nature management"*, Poligrafist, Khanty-Mansiysk, pp. 195-201, 2008.

[11] A.V.Filatov and A.V.Yevtyushkin, "Estimation of Earth surface displacements in area of intensive oil production in West Siberia by InSAR using ENVISAT\ASAR", *Proceedings of VI Opened All-Russia Conference "Current aspects of remote sensing of Earth from space"*, Moscow, 2009.

[12] A. Ferretti, C. Prati, F. Rocca, "Permanent scatterers in SAR interferometry", *Proc. Int. Geosci. Remote Sensing Symp.*, Hamburg, Germany, June 28 – July 2 1999, pp. 705-715, Mar. 1999.

[13] Ferretti, C. Prati, F. Rocca, "Non-linear subsidence rate estimation using permanent scatterers in differential SAR interferometry", *IEEE Trans. Geosci. Remote Sensing*, vol. 38, pp. 2202-2212, Sept. 2000.

[14] B.M. Kampes, "Radar Interferometry: Persistent Scatterer Technique", Springer, Dordrecht, 212p., 2006.

[15] A.V.Filatov and A.V.Yevtyushkin. "InSAR technology for DEM construction and displacement estimation", *Bulletin of Novosibirsk State University*, Novosibirsk State University, Novosibirsk, pp. 66-72, 2009.

[16] Y.V. Vasilev, O.S. Martynov, A.V. Radchenko, "Analysis of research results on Samotlor geodynamic polygon", *Proceedings of 8th Science and Practical Conference "Routes of realization of oil and gas potential of KHMAO region"*, IzdatNaukaService, Khanty-Mansiysk, pp. 452-461, 2005.

[17] A.V. Filatov, A.V. Yevtyushkin, "Estimation of ground surface displacements by radar interferometry in the condition of high temporal decorrelation", *Proceedings of 16th International Symposium "Atmospheric and Oceanic Optics"*, Institute of Atmospheric Optics, Tomsk, pp. 587-589, 2009.

[18] A.V. Filatov and A.V. Yevtyushkin, "Detection of ground surface displacements in area of intensive oil and gas production by InSAR data", *Proceedings of the ESA Living Planet Symposium. 28 June - 2 July 2010*, ESA SP-686, ESA Communications, Noordwijk, December 2010.

[19] A.V. Filatov and A.V. Yevtyushkin. "Detection of displacements of oil production objects by radar interferometry", *Thesis of VI Opened All-Russia Conference "Current aspects of remote sensing of Earth from space"*, [Online] http://d902.iki.rssi.ru/theses-cgi/thesis.pl?id=2172, Moscow, 2010.